12

Structural DNA Nanotechnology

An Overview

Nadrian C. Seeman

Summary

Structural DNA nanotechnology uses unusual DNA motifs to build target shapes and arrangements. These unusual motifs are generated by reciprocal exchange of DNA backbones, leading to branched systems with many strands and multiple helical domains. The motifs may be combined by sticky-ended cohesion, involving hydrogen bonding or covalent interactions. Other forms of cohesion involve edge sharing or paranemic interactions of double helices. A large number of individual species have been developed by this approach, including polyhedral catenanes, such as a cube and a truncated octahedron; a variety of single-stranded knots; and Borromean rings. In addition to these static species, DNA-based nanomechanical devices have been produced that are targeted ultimately to lead to nanorobotics. Many of the key goals of structural DNA nanotechnology entail the use of periodic arrays. A variety of two-dimensional DNA arrays have been produced with tunable features, such as patterns and cavities. DNA molecules have been used successfully in DNA-based computation as molecular representations of Wang tiles, whose self-assembly can be programmed to perform a calculation. Structural DNA nanotechnology appears to be at the cusp of a truly exciting explosion of applications, which can be expected to occur by the end of the current decade.

Key Words

Holliday junctions; branched DNA; DNA nanotechnology; sticky-ended cohesion; double crossover molecules; triple crossover molecules; paranemic cohesion; edge sharing; reciprocal exchange; DNA complementarity.

1. Introduction

The year 2003 is the 50th anniversary of the Watson-Crick ***(1)*** model for double helical DNA. The impact of this model during the past half century has been immense. Indeed, the double helix has become a cultural icon of our

From: *Methods in Molecular Biology, vol. 303: NanoBiotechnology Protocols*
Edited by: S. J. Rosenthal and D. W. Wright © Humana Press Inc., Totowa, NJ

civilization in much the same way that the pyramids of Egypt, the temples of Greece, the cathedrals of medieval Europe, and the Great Wall of China were icons of previous eras. The simplicity and elegance of the molecule that nature evolved to perpetuate and express genetic information, have revolutionized genetics and have had a similar impact in other areas ranging from medicine to forensics. All of these applications are predicated on the complementarity of the two strands of DNA, rooted in the hydrogen-bonded base pairing between adenine (A) and thymine (T) and between guanine (G) and cytosine (C). The DNA double helix is inherently a nanoscale object; its diameter is about 20 Å (2 nm) and the separation of the bases is 3.4 Å; the helical periodicity is 10–10.5 nucleotide (nt) pairs per turn, or approx 3.5 nm per turn. Here, I discuss making complex materials with nanoscale features from DNA; this pursuit is termed *structural DNA nanotechnology*.

What purposes would be served by producing DNA-based constructs? It is expected that these systems can be applied to several practical ends. The initial motivating goal for this research is that spatially periodic networks are crystals. If stick-figure crystalline cages can be built on the nanometer scale, they could be used to orient other biological macromolecules as guests inside those cages, thereby rendering their three-dimensional (3D) structures amenable to diffraction analysis ***(2)***. This notion is illustrated in **Fig. 1A**, which shows a DNA "box" hosting macromolecular guests. Similarly, the same types of crystalline arrays could be used to position and orient components of molecular electronic devices with nanometer-scale precision ***(3)***. An example of this type of application is shown in **Fig. 1B**. Two DNA branched junctions have pendent from them a nanowire. When their sticky ends cohere, the nanowires are organized as well. DNA-based nanomechanical devices can lead to a nanometer-scale robotics and to very smart materials, materials that respond to specific stimuli by particular spatial transitions. Structural DNA nanotechnology creates motifs that can be useful for DNA-based computation and for the algorithmic assembly of materials ***(4)***. Algorithmic assembly holds great promise for the highly controlled construction of materials with designed features and target sizes in one, two, or three dimensions.

A key, if often unnoticed, feature of the double helix is that its axis is linear, not in the geometric sense of being a straight line, but in the topological sense that it is unbranched. The biological relevance of this fact is that only a linear complement to a DNA strand is well defined ***(5)***. This point is illustrated in **Fig. 2**. In **Fig. 2A**, a DNA duplex molecule is illustrated, in which each base of strand 2 is paired to strand 1. By contrast, **Fig. 2B** shows a molecule in which strand 2 contains a hairpin that produces a 3-arm branched junction. Every base in strand 1 has a complement in strand 2, just as in **Fig. 2A**. However, the complement is not well defined. The third (horizontal) arm of the junction could have

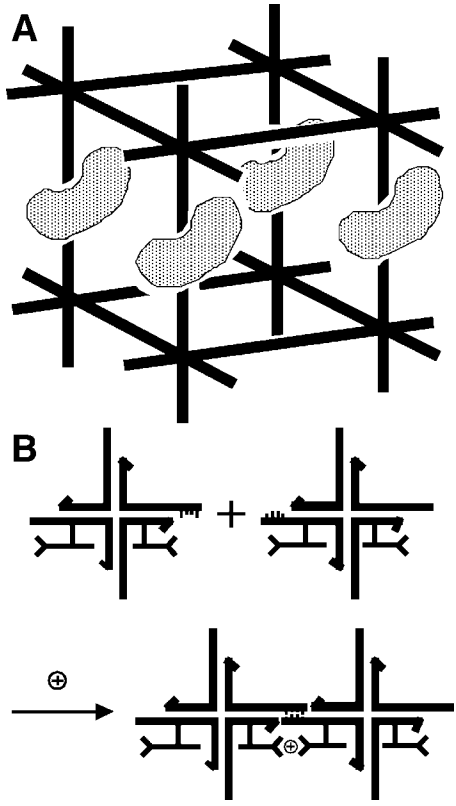

Fig. 1. Applications of DNA periodic arrays. **(A)** Biological macromolecules organized into a crystalline array are depicted. A cubelike box motif is shown, with sticky ends protruding from each vertex. Attached to the vertical edges are biological macromolecules that have been aligned to form a crystalline arrangement. The idea is that the boxes are to be organized into a host lattice by sticky ends, thereby arranging the macromolecular guests into a crystalline array, amenable to diffraction analysis. **(B)** Nanoelectronic circuit components organized by DNA are deposited. Two DNA branched junctions are shown, with complementary sticky ends. Pendent from the DNA are molecules that can act as molecular wires. The architectural properties of the DNA are seen to organize the wirelike molecules, with the help of a cation, which forms a molecular synapse.

any length, without affecting the complementarity of strand 2 for strand 1. Thus, the replication protocol used by DNA polymerase would not be effective in replicating this structure exactly, even though it would produce complements to the individual strands. Nevertheless, biology does use branched DNA as ephemeral intermediates in the processes of replication, recombination, and repair.

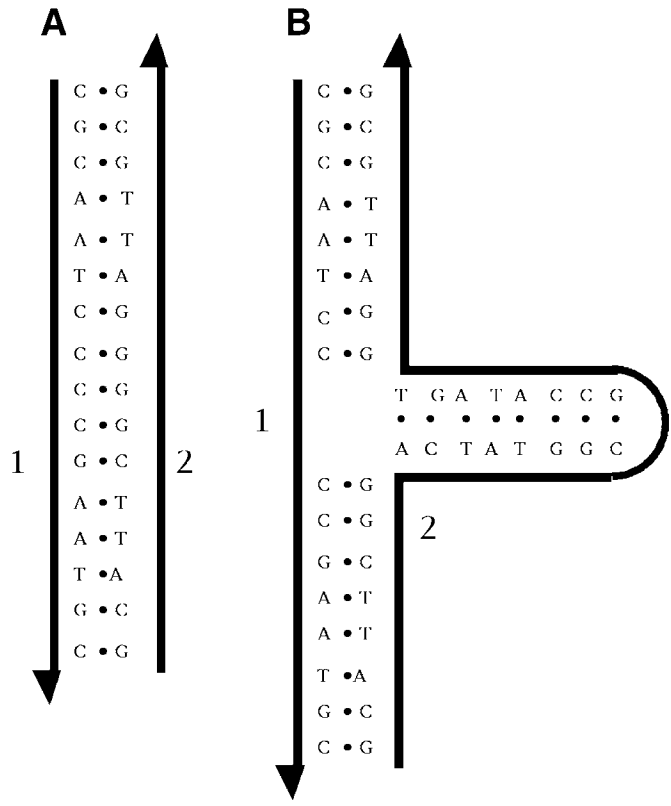

Fig. 2. Inexact complementarity in branched DNA. **(A)** A DNA duplex with its strands numbered 1 and 2 is shown. **(B)** A 3-arm branched junction with its strands also labeled 1 and 2 is shown; strand 1 is identical to strand 1 in (A). Every nucleotide of strand 1 in (B) is complemented by a nucleotide in strand 2 in (B), but there are many nucleotides in the branch whose sequences are irrelevant to the complementarity between strands 2 and 1. The only well-defined complement to strand 1 is strand 2 of (A).

Regardless of the difficulties that branched DNA might present as genetic material, it is extremely valuable for structural DNA nanotechnology, because linear DNA molecules do not lead to inherently interesting arrangements of DNA in two or three dimensions. Genetic engineers have used sticky-ended cohesion and ligation for nearly 30 yr to produce linear recombinant DNA molecules ***(6)***. These molecules are of value for their sequences and the gene products to which they can lead, but structurally speaking, they consist of long lines or circles, perhaps including some catenanes or knots. However, if one combines sticky-ended cohesion with branched DNA species, it is possible to

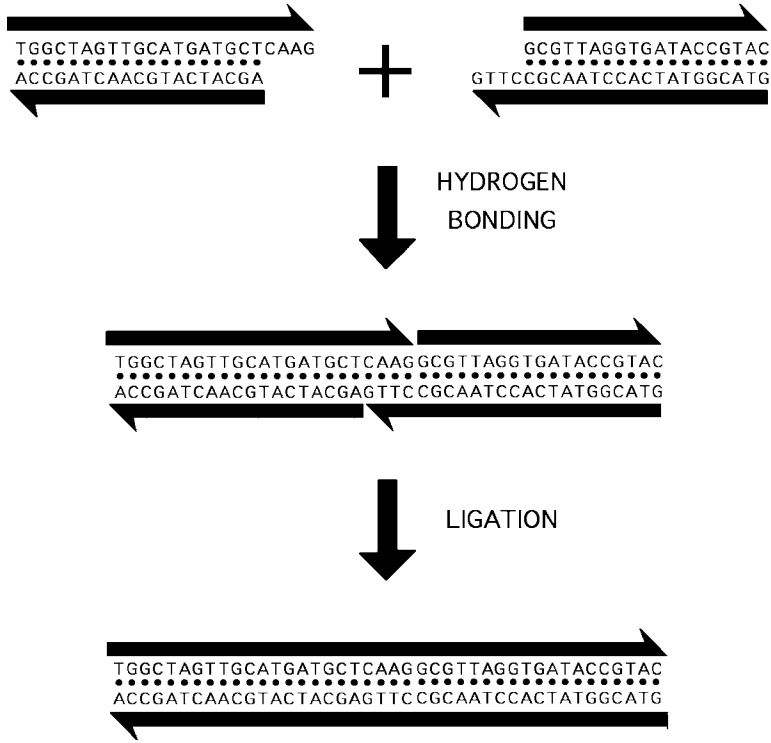

Fig. 3. Sticky-ended cohesion. **(Top)** Two linear double helical molecules of DNA are shown. The black lines terminating in half arrows indicate the antiparallel backbones. The half-arrows also indicate the 5′→3′ directions of the backbones. The right end of the left molecule and the left end of the right molecule have single-stranded extensions ("sticky ends") that are complementary to each other. **(Middle)** Under the proper conditions, these molecules bind to each other specifically by hydrogen bonding. **(Bottom)** The molecules can be ligated to covalency by the proper enzymes and cofactors.

produce many complex structures and topologies with relatively little effort. **Figure 3** illustrates the nature of sticky-ended cohesion: two double helices with complementary single-stranded overhangs will cohere to form a complex under the appropriate solution conditions.

The recognition of one strand of DNA by another strand is common to many types of DNA nanotechnology and to molecular biology. The special feature of *structural* DNA nanotechnology is that it takes advantage of the well-defined structure at the point where the two helices cohere. **Figure 4** shows the crystal structure of a DNA decamer that forms continuous helices within the periodic lattice *(7)*. In contrast to many other crystals of DNA decamers, these decamers

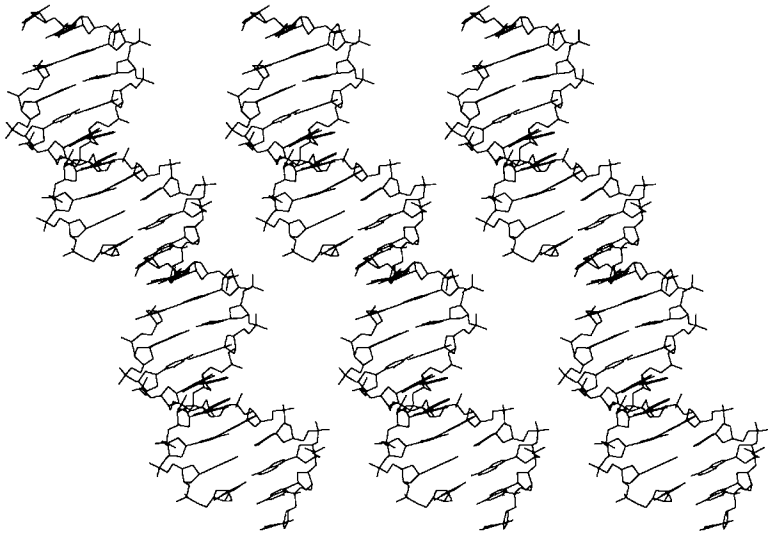

Fig. 4. Crystal structure of infinite DNA helices held together by sticky ends. Shown are three DNA double helices that consist of an infinite repeat of a decamer. The decamers are held together by complementary sticky ends, flanked by breaks in the DNA backbone. The key point is that the DNA around the sticky ends is the same as the rest of the DNA; it is all B-DNA, so the structure of any sticky-ended complex is known with high precision.

are held together by sticky ends at their 5′ ends. The key point of the crystal structure is that the 3D conformation of the DNA in the vicinity of the sticky end is the same as the rest of it; it is all B-DNA, the classic structure. Thus, if two DNA molecules are held together by sticky ends, and one knows the coordinates of one of them, then one knows the coordinates of the one to which it is binding by sticky-ended cohesion. This fact is exploited extensively in structural DNA nanotechnology. If one wished to use some other biologically based recognition system, such as antibody-antigen interactions, it would be possible, but one would have to work out the spatial relationships of the two partners in the binding reaction for every pair, say, by a crystal structure. By contrast, the many possible DNA sticky ends (4^N for N-base sticky ends) have structures that are virtually identical. Other modes of cohesion are being introduced into structural DNA nanotechnology. These include paranemic crossover (PX) cohesion ***(8)*** and edge sharing ***(9)***. However, the structural parameters of these forms of cohesion can only be estimated at this time.

It is easy to generate branched DNA molecules by the logic used in biological systems—reciprocal exchange of strands ***(10)***. An example of reciprocal

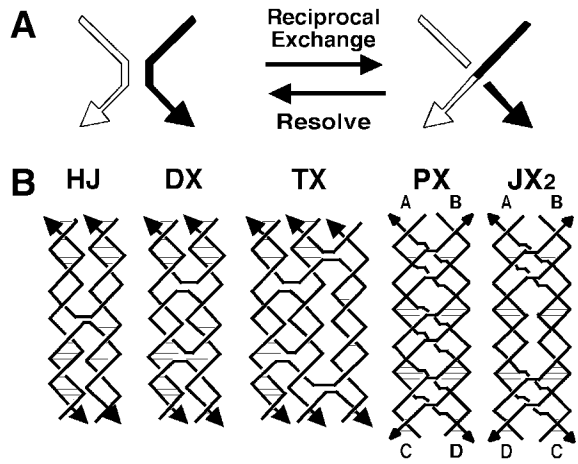

Fig. 5. Motif generation and sample motifs. **(A)** Reciprocal exchange of DNA backbones. Two strands are shown on the left, one filled and one unfilled. Following reciprocal exchange, one strand is filled-unfilled, and the other strand is unfilled-filled. **(B)** Key motifs in structural DNA nanotechnology. On the left is an HJ, a 4-arm junction that results from a single reciprocal exchange between double helices. To its right is a DX molecule, which results from a double exchange. To the right of the DX is a TX molecule, which results from two successive double reciprocal exchanges. The HJ and the DX and TX molecules all contain exchanges between strands of opposite polarity. To the right of the TX molecule is a PX molecule, where two double helices exchange strands at every possible point where the helices come into proximity. To the right of the PX molecule is a JX_2 molecule that lacks two of the crossovers of the PX molecule. The exchanges in the PX and JX_2 molecule are between strands of the same polarity.

exchange is shown in **Fig. 5A**, where a filled strand and an outlined strand trade portions of their strands. **Figure 5B** illustrates a number of motifs derived in this fashion that have proved to be important in structural DNA nanotechnology. At the left is the Holliday junction (HJ), the biological intermediate in genetic recombination ***(11)***, which results from a single reciprocal exchange between double helices. To its right is the double crossover (DX) molecule ***(12)***, an intermediate in meiosis ***(13)***, which is derived by two exchanges between double helices. On the right of the DX molecule is the triple crossover (TX) molecule, which is generated by two reciprocal exchanges between a helix of the DX molecule and another double helix ***(14)***. The two strands of the double helix have opposite polarities. Exchange can occur between strands of the same polarity or strands of opposite polarity. The HJ, DX, and TX molecules shown are all illustrated to have been the result of exchanges between

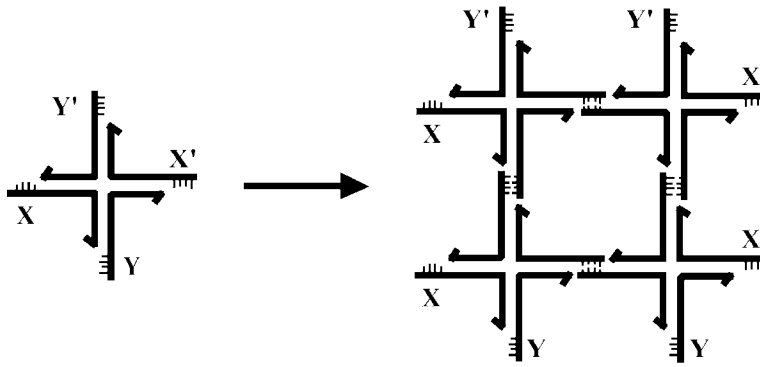

Fig. 6. Combination of branched motifs and sticky ends. At the left is a 4-arm branched junction with sticky ends, labeled X and its complement X′, and Y and its complement Y′. On the right, four such molecules are combined to produce a quadrilateral. The sticky ends on the outside of the quadrilateral are available so that the structure can be extended to form a 2D lattice.

strands of opposite polarity. The PX structure on the right of the TX molecule illustrates crossovers between strands of the same polarity ***(10)***. Exchange in the PX motif occurs at every possible point where the strands are juxtaposed. The JX_2 variant to the right of the PX molecule lacks two crossovers in the middle; it has been used in a robust nanomechanical device ***(15)***.

Figure 6 illustrates the HJ single crossover junction structure in a convenient branched arrangement, much like the intersection of two roads. Each of the four double helical arms has been tailed by a sticky end. The arrangement on the right shows four of these junctions assembled to form a quadrilateral by sticky-ended cohesion. In addition to the sticky ends that pair within each edge of the quadrilateral, sticky ends are visible on the outside of the structure, so that this arrangement could be extended to yield two-dimensional ***(20)*** crystalline arrays. It is important to realize that the parallel-line representation of DNA used in **Fig. 6** is only a convenience. The double helical nature of DNA really makes this a 3D system, rather than a 2D system. Thus, in principle, branched DNA molecules tailed in sticky ends can be assembled into 3D objects and lattices.

Why use DNA for this purpose? The key reason has already been discussed: sticky-ended cohesion of DNA is the most predictable *intermolecular* interaction of any known molecular system, in the senses of affinity, diversity, and structure. In addition, convenient automated chemistry exists for the synthesis of DNA molecules of particular sequences, both conventional nucleotides and specially derivatized variants, such as biotinylated nucleotides or branched

residues. There are numerous enzymes that can be used with DNA: ligases to join cohesive ends covalently ***(6)***, restriction enzymes that can be used both synthetically ***(16)*** and analytically ***(17,18)***, exonucleases for the removal of failure products ***(17)***, and topoisomerases that can be used to diagnose topological problems ***(19)***. DNA is a relatively stiff molecule, with a persistence length of about 50 nm under standard conditions ***(20)***. There is an external code on DNA so that its sequence may be read from the grooves, even though the double helix is intact ***(21)***. The functional group density of DNA is very high; thus, it may be derivatized at a density limited only by the nucleotide repeat. In addition, the gene therapy and antisense enterprises have produced large numbers of variants on the theme of DNA (e.g., *see* **ref. *22***); although it is most convenient to prototype nanoconstructs with DNA, many applications are likely to benefit from the use of variants such as peptide nucleic acids ***(23)***.

How does one choose sequences for DNA constructs? The key to any successful molecular engineering approach is to design the components of a construction not just so that they are capable of yielding the product, but also to ensure, insofar as possible, that no other product will be competitive with the target. Ultimately, one must estimate the thermodynamics of all possible sequences and select the one most likely to lead to the intended product ***(24)***. Empirically, I have found that adequate sequences can be generated by the approximation to this approach called sequence symmetry minimization, which is shown in **Fig. 7** ***(2,25)***. This drawing illustrates a 4-arm junction; its arms are each 8 nt long, so each of its strands contains 16 nt. One divides the 16 nt into a series of overlapping elements (13 tetramers in this case). One insists that each of these elements, such as the boxed CGCA and GCAA, be unique. In addition, one also insists that any element that spans a bend (such as the boxed CTGA) not have its simple contiguous Watson-Crick complement (TCAG) anywhere in the sequence. With these constraints, competition with the target octamers can come only from trimers, such as the ATG sequences in the dashed boxes. It should be clear that this approach assumes that double helices are the most favorable structures that DNA can form, and that maximizing double helix formation will lead to the successful formation of branch points. The success of this method relies on the cooperativity of DNA double helix formation.

2. DNA Objects

Individual branched junctions have been constructed containing 3 ***(26)***, 4 ***(24)***, 5, and 6 arms ***(27)***. A variety of studies have shown that the angles between the arms appear to be flexible ***(26,28,29)***. Consequently, the earliest constructions consisted of topological targets, rather than targets with specific 3D geometries. Both the level of control and the proofs of these structures are on the topological level. The connectivity of an object is the number of vertices

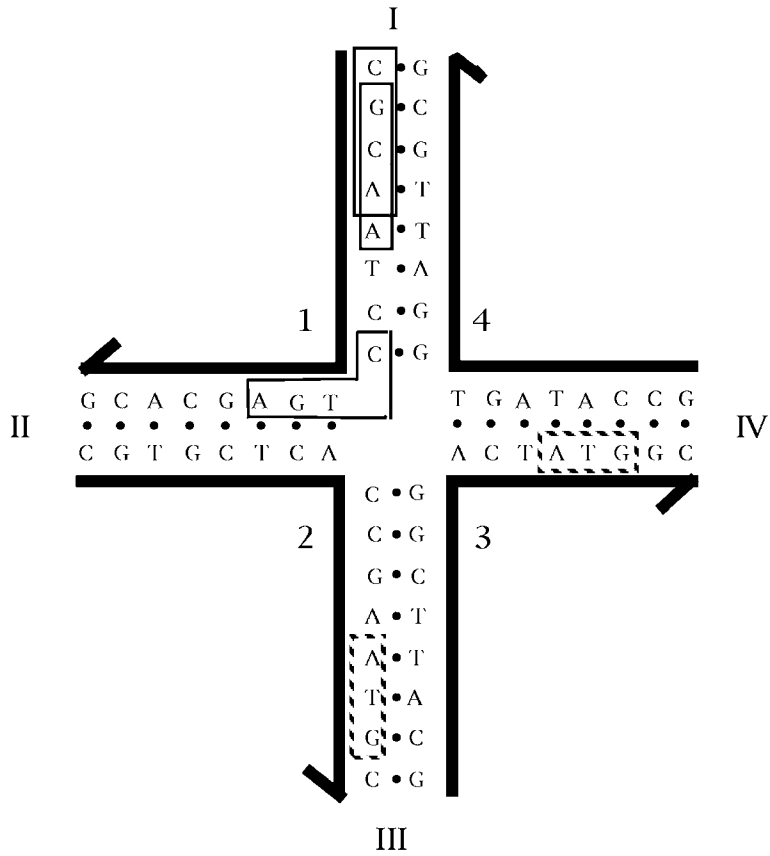

Fig. 7. Sequence Symmetry Minimization produces a stable DNA branched junction. The junction shown is composed of four strands of DNA, labeled with Arabic numerals. The half arrows indicate the 3′ end of each strand. Each strand is paired with two other strands to form double helical arms; the arms are numbered with Roman numerals. The dots between the bases indicate the hydrogen-bonded base paring that forms the double helices. The sequence of this junction has been optimized to minimize symmetry and non-Watson-Crick base pairing. Because there is no homologous twofold sequence symmetry flanking the central branch point, this junction cannot undergo the branch migration isomerization reaction. At the upper part of arm I, two of the 52 unique tetrameric elements in this complex are boxed; these are CGCA and GCAA. At the corner of strand 1, the sequence CTGA is boxed. This is 1 of 12 sequences in the complex (3 on each strand) that span a junction. The complements to each of these 12 sequences are not present. Whereas tetrameric elements have been used to assign the sequence of this molecule, there is redundancy in the molecule among trimers, such as the ATG sequences shown in the dashed boxes.

to which every vertex is bonded via the edges. The first object with a nontrivial connectivity of 3 or greater was a DNA molecule whose helix axes were connected like the edges of a cube ***(17)***. The edges consisted of DNA double helices, and the vertices corresponded to the branch points of 3-arm junctions. There were two turns per edge, so each face consisted of a cyclic single strand linked twice to each of its four neighbors, forming a hexacatenane. Every edge of this molecule (shown in **Fig. 8A**) contains a unique restriction site. It was constructed in solution, and proof of synthesis consisted of restricting the final hexacatenane to target subcatenanes ***(17,30)***.

In the next development, a truncated octahedron was also constructed from DNA ***(18)***, this time using a solid-support-based method ***(16)***. This molecule (shown in **Fig. 8B**) is also a complex catenane. There are 14 faces to a truncated octahedron, so this molecule is a 14-catenane, with six strands corresponding to square faces and eight strands corresponding to hexagonal faces. Although the truncated octahedron is a 3-connected object, it was constructed with 4-arm junctions (not shown), in the hope that the extra helices could be used to connect the polyhedra into a macromolecular version of zeolite A. Enough material was produced to demonstrate the synthesis, but not to use it as starting material for lattice construction.

In addition to these polyhedral catenanes, a series of strictly topological targets has been produced. Knots and catenanes are characterized by the set of nodes seen when they are projected into a plane. The half turn of DNA corresponds to such a node in any topological target. Consequently, it is easy to produce virtually any knot from DNA, with negative nodes being produced by conventional right-handed B-DNA and positive nodes being derived from left-handed Z-DNA ***(31)***. **Figure 8C** illustrates a trefoil knot with negative nodes, and **Fig. 8E** a trefoil knot with positive nodes. **Figure 8D** shows a figure-8 knot with two negative nodes and two positive nodes. All of these knots (and an unknotted circle) have been produced from one strand of DNA by changing ligation conditions. The strand contained two regions that could turn into Z-DNA, but with different propensities: at non-Z-promoting conditions, the knot with negative nodes was produced; at conditions that weakly promote the B-Z transition, the figure-8 knot was produced; and at strongly Z-promoting conditions, the trefoil with positive nodes was produced ***(32)***. **Figure 8F** illustrates Borromean rings built from the combination of a right-handed B-DNA 3-arm junction connected to a left-handed Z-DNA 3-arm junction ***(33)***. Borromean rings have a special property: when any ring in a set of Borromean rings is cut, all the rings fall apart. This is an extremely difficult topology to produce from conventional organometallic systems, but it was relatively easy to make it from DNA.

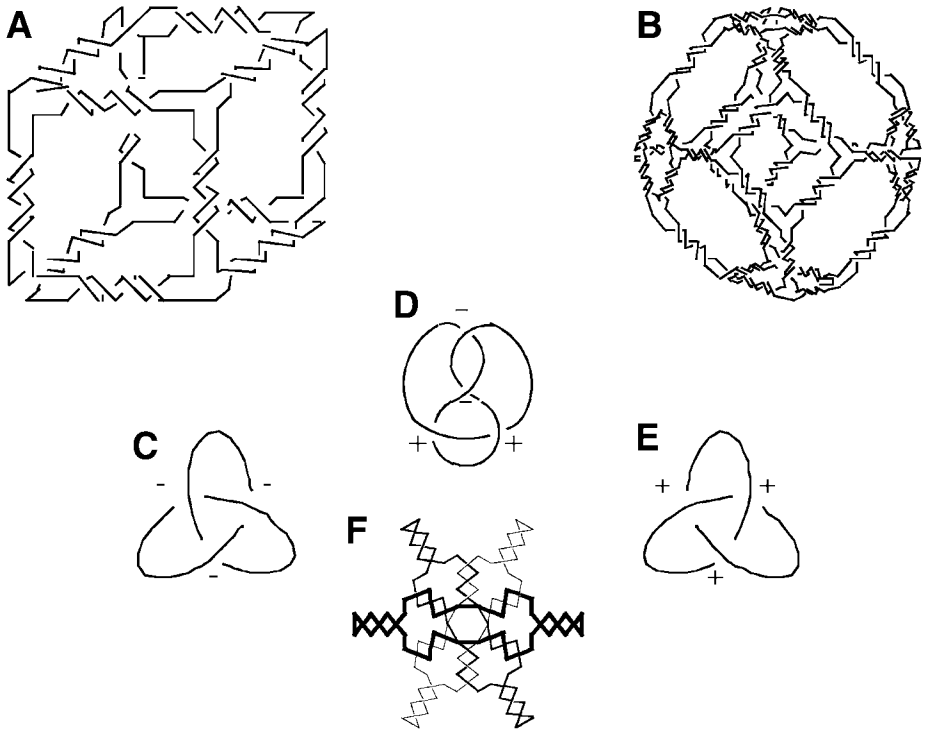

Fig. 8. Ligated products from flexible DNA components. **(A)** Stick cube and **(B)** stick truncated octahedron. The drawings show that each edge of the two figures contains two turns of double helical DNA. The twisting is confined to the central portion of each edge for clarity, but it actually extends from vertex to vertex. Both molecules are drawn as though they were constructed from 3-arm junctions, but the truncated octahedron has been constructed from 4-arm junctions, which has been omitted for clarity. **(C–E)** Deliberate knots constructed from DNA. The signs of the nodes are indicated: (C) a trefoil knot with negative nodes; (D) a figure-8 knot; (E) a trefoil knot with positive nodes. **(F)** Borromean rings. Scission of any of the three rings shown results in the unlinking of the other two rings.

3. DNA Arrays

Being able to produce a series of topological targets, such as the knots, Borromean rings and polyhedral catenanes are of interest, but the greatest value will be derived when a variety of species can be attached to each other, particularly if functionality is associated with them. The essence of structural DNA nanotechnological goals is to place specific functional species at particular loci, using the architectural properties of DNA. Functionality includes the use of periodic DNA arrays to scaffold molecular arrangements in other species,

alogorithmic assemblies that perform computations, and the development of DNA-based nanomechanical devices.

In addition to the intermolecular specificity described in **Subheading 1.**, the key architectural property that is needed to build and demonstrate these arrays and devices is high structural integrity in the components; even if their associations are precise, the assembly from marshmallow-like components will not produce well-structured materials. As noted above, single-branched junctions, such as the HJ structure in **Fig. 6**, are relatively flexible. Fortunately, the DX molecule is considerably more rigid, apparently stiffer than double helical DNA ***(34,35)***. The TX and PX molecules appear to share this rigidity ***(14,15)***. Consequently, it has been possible to use these molecules as the building blocks of both arrays and devices. Arrays are expected to be useful as the scaffolding for the heteromolecules shown in **Fig. 1**, as the basis of DNA computation by self-assembly, and as frameworks to mount DNA nanomechanical devices.

Figure 9 illustrates 2D arrangements that entail the use of DX molecules to produce periodic patterns. **Figure 9A** illustrates a two-component array that can tile the plane. One tile is a DX molecule labeled **A** and the second is a DX molecule labeled **B***. **B*** contains another DNA domain that projects out of the plane of the helix axes. This other domain can serve as a topographic marker for the atomic force microscope when the **AB*** array is deposited onto the surface of mica. The dimensions of the two DX tiles in **Fig. 9A** are about 4 nm high × 16 nm wide × 2 nm thick. Thus, the **B*** markers in the 2D array shown should appear as stripelike features separated by approx 32 nm, which has been confirmed by experiment. **Figure 9b** shows a four-tile arrangement that should produce stripes separated by approx 64 nm, also confirmed by experiment ***(36)***. Thus, it is possible to design and produce patterns using DNA components; these patterns contain predictable features, based on the sticky-ended cohesion of individual motifs. The patterns can be modified by the enzymatic addition or removal of these features; nonenzymatic addition has also been demonstrated ***(37)***. In addition to forming arrays from DX molecules, it is possible to produce periodic arrays from TX molecules ***(14)***. A variety of DNA parallelograms also have been used to produce 2D arrays ***(38–40)***. These motifs are produced by combining four HJ-like branched junctions. Unlike the DX, TX, and PX molecules, the two domains of the HJ molecule are not parallel to each other. As a function of the sequence and backbone connections at the crossover point, they adopt angles of approx 60° ***(38)***, approx –70° ***(39)***, or approx 40° ***(40)***, thus producing a diversity of parallelogram angles.

4. DNA Nanomechanical Devices

Nanomechanical action is a central target of nanotechnology. The first DNA-based devices were predicated on structural transitions of DNA driven by small

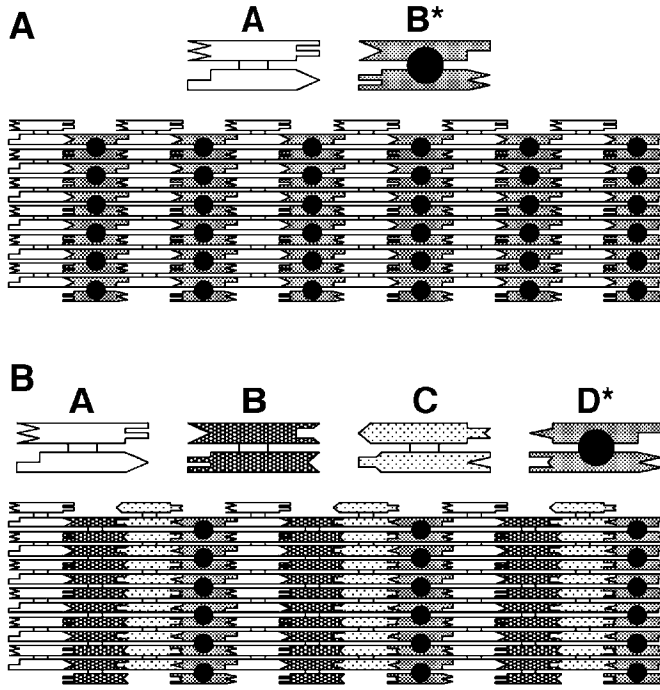

Fig. 9. Tiling the plane with DX molecules. **(A)** Two-tile pattern. The two helices of the DX molecule are represented schematically as rectangular shapes that terminate in a variety of shapes. The terminal shapes are a geometrical representation of sticky ends. The individual tiles are shown at the top of the figure; the way tiles fit together using complementary sticky ends to tile the plane is shown at the bottom. The molecule labeled **A** is a conventional DX molecule, but the molecule labeled **B*** contains a short helical domain that protrudes from the plane of the helix axes; this protrusion is shown as a black dot. The black dots form a stripelike feature in the array. The dimensions of the tiles are 4×16 nm in this projection. Thus, the stripelike features should be about 32 nm apart. **(B)** Four-tile pattern. The same conventions apply as in **(A)**. The four tiles form an array in which the stripes should be separated by about 64 nm, as confirmed by atomic force microscopy.

molecules. The initial DNA device entailed the extrusion of a DNA cruciform structure from a cyclic molecule ***(41)***. The system consisted of a DNA circle (approx 300 nt) that contained a branch point capable of assuming five different positions, because there were four symmetric nucleotides at its base; the symmetry was eliminated beyond that point. The device is illustrated in **Figure 10**. The position of the branch point was controlled by the addition or removal of an intercalating dye that changes the supercoiling. This system was not very

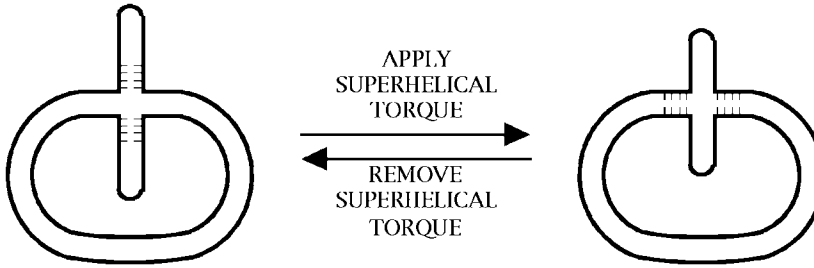

Fig. 10. Torsionally driven DNA device. On the left is a DNA circle that contains a fixed branch. There are four symmetric nucleotide pairs at the base of the branch, and these can undergo branch migration. With the normal twist of the DNA in the circle, the nucleotides are extruded from the circle. However, when the twist is decreased by the addition of ethidium, the nucleotide branch migrates to become part of the circle.

convenient to operate, and the large size of the DNA circle made it unwieldy to handle. Nevertheless, it demonstrated that DNA could form the basis of a two-state mechanical system.

The second DNA-based device (**Fig. 11A**) was a marked advance. It was relatively small and included two rigid components, DX molecules like those used to make the arrays in **Fig. 9**. The basis of the device was the transition between right-handed (conventional) B-DNA and left-handed Z-DNA. There are two requirements for the formation of Z-DNA: a "proto-Z" sequence capable of forming Z-DNA readily (typically a $[CG]_n$ sequence), and conditions (typically high salt or molecules like $Co[NH_3]_6^{3+}$ that emulate the presence of high salt) to promote the transition ***(42)***. The sequence requirement provides control over the transition in space, and the requirement for special conditions provides control over the transition in time. As shown in **Fig. 11A**, the device consists of two DX molecules connected by a $(CG)_{10}$ double helical shaft that provides the proto-Z sequence. In B-promoting conditions, both of the DX helices not collinear with the shaft are on the same side of the shaft. In Z-promoting conditions, one of these helices ends up on the other side of the shaft. This difference is the result of converting a portion of the shaft to Z-DNA, which rotates one DX motif relative to the other by 3.5 turns. The movement was demonstrated by fluorescence resonance energy transfer (FRET) measurements that respond to the difference between dye separations on the DX motifs ***(43)***.

The reason that the B-Z device is not the ultimate DNA-based nanomechanical device is that it is activated by an unspecific molecule, $Co(NH_3)_6^{3+}$. Consequently, a number of such devices, embedded in an array, would all respond similarly, although some chemical nuance might be available to obtain

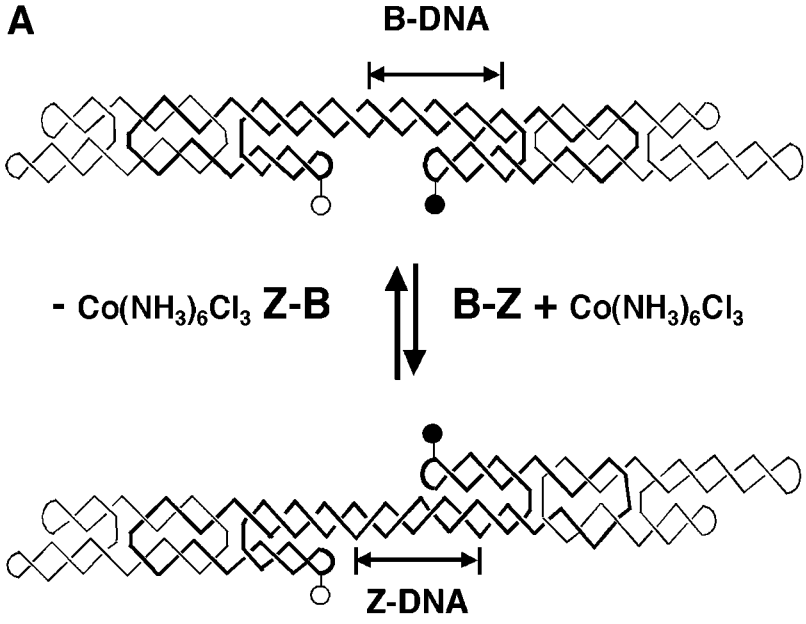
A
B-DNA
- Co(NH3)6Cl3 Z-B
B-Z + Co(NH3)6Cl3
Z-DNA

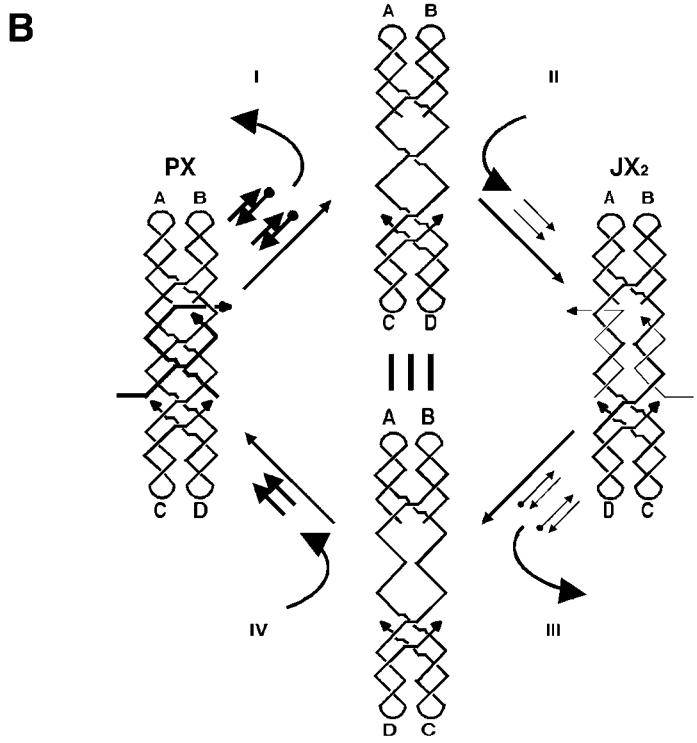
B
A B
I
II
PX
JX2
A B
C D
C D
A B
A B
D C
D C
IV
III

differential responses ***(32)***. Thus, N two-state devices would result in essentially two structural states; clearly it would be of much greater utility to have N distinct two-state devices capable of producing 2^N structural states. It is evident that a sequence-dependent device would be an appropriate vehicle for the goal of achieving multiple states; Yurke et al. ***(44)*** worked out the method for manipulating sequence-dependent devices. It entails setting the state of a device by the addition of a "set" strand that contains an unpaired tail. When the full complement to the set strand is added, the set strand is removed, and a different set strand may be added. This system has been adapted to the PX and JX_2 motifs (**Fig. 5**) ***(15)***. **Figure 11B** shows how these two states can be interconverted by the removal of one pair of set strands (processes I and III) and the addition of the opposite pair (processes II and IV). The tops and bottoms of the two states differ by a half rotation, as seen by comparing the A and B labels at the tops of the molecules, and the C and D labels at the bottoms of the molecules. A variety of devices can be produced by changing the sequences of the regions where the set strands bind.

Fig. 11. *(See opposite page)* DNA-based nanomechanical devices. **(A)** Device predicated on B-Z transition. The molecule consists of two DX molecules, connected by a segment containing proto-Z-DNA. The molecule also consists of three cyclic strands, two on the ends, drawn with a thin line, and one in the middle, drawn with a thick line. The molecule contains a pair of fluorescent dyes to report their separation by FRET. One is represented as a solid circle, and the other as an open circle. In the upper molecule, the proto-Z segment is in the B conformation, and the dyes are on the same side of the central double helix. In the lower molecule, the proto-Z segment is in the Z conformation, and the dyes are on opposite sides of the central double helix. At the top and bottom, the two vertical lines flanking the conformation descriptor indicate the length of the proto-Z-DNA and its conformation. **(B)** Sequence-dependent device. This device uses two motifs, PX and JX_2. The labels A, B, C, and D on both show that there is a 180° difference between the wrappings of the two molecules. Two strands are drawn as thick lines at the center of the PX motif, and two strands are drawn with thin lines at the center of the JX_2 motif; in addition to the parts pairing to the larger motifs, each has an unpaired segment. These strands can be removed and inserted by the addition of their total complements (including the segments unpaired in the larger motifs) to the solution; these complements are shown in processes I and III as strands with black dots (representing biotins) on their ends. The biotins can be bound to magnetic streptavidin beads so that these species can be removed from solution. Starting with the PX, one can add the complement strands (process I), to produce an unstructured intermediate. Adding the set strands in process II leads to the JX_2 structure. Removing them (III) and adding the PX set strands (IV) completes the machine cycle. Many different devices could be made by changing the sequences to which the set strands bind.

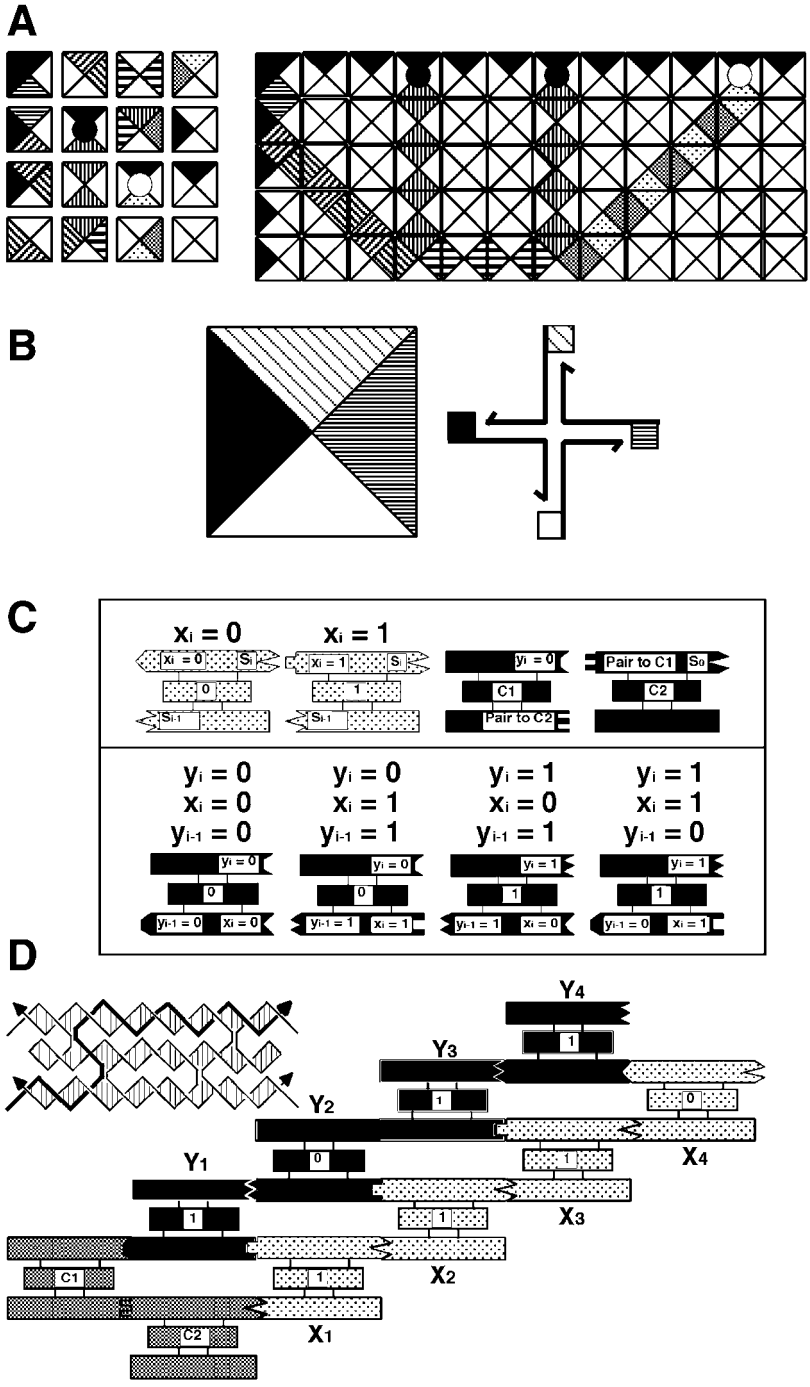
A
B
C
$x_i = 0$
$x_i = 1$
$y_i = 0$
Pair to C1
C1
C2
Pair to C2
$y_i = 0$ $x_i = 0$ $y_{i-1} = 0$
$y_i = 0$ $x_i = 1$ $y_{i-1} = 1$
$y_i = 1$ $x_i = 0$ $y_{i-1} = 1$
$y_i = 1$ $x_i = 1$ $y_{i-1} = 0$
D
Y_4
Y_3
Y_2
Y_1
X_4
X_3
X_2
X_1
C1
C2

5. DNA-Based Computation

In 1994, Leonard Adleman ***(45)*** founded experimental DNA-based computation. His approach is different from the use of DNA to scaffold nanoelectronic component assembly, suggested in **Fig. 1**. Instead, Adleman combined the information in DNA molecules themselves, using standard biotechnological operations (ligation, polymerase chain reaction, gel electrophoresis, and sequence-specific binding to derivatized beads) to solve a Hamiltonian path problem. This is a problem related to the traveling salesman problem (What is the optimal route for a salesman to visit *N* cities?). In the Hamiltonian path problem, there is a defined start point and end point, and an incomplete set of routes between the cities; the problem is to establish whether there is a path between the start point and end point that visits all the cities. The idea behind DNA-based computation is that there exist certain classes of computational problems for which the parallelism of molecular assembly overcomes the slow speed of the required macroscopic manipulations. Many varieties of DNA-based computation have been proposed, and a number of them have been tested experimentally for relatively small cases. Space does not permit discussion of all of them.

Nevertheless, there is one approach to DNA-based computation that is relevant to our discussion of structural DNA nanotechnology. This was a method

---

Fig. 12. *(see opposite page)* DNA-based computation. **(A)** Wang tiles. On the left is a group of 16 Wang tiles. The edges of the tiles are flanked by a variety of patterns. These tiles assemble into the mosaic on the right according to the rule that each edge in the mosaic is flanked by the same pattern. The mosaic represents a calculation, adding 4 to 7 to obtain 11. The two addends are in the top row in the fourth and seventh column. The path through the calculation begins in the upper left corner and continues on a diagonal until it encounters the vertical column in the fourth column. The path then switches to horizontal until the seventh column and then switches again to the diagonal, terminating in the eleventh column. (After **ref. *46***.) **(B)** Relationship between Wang tiles and branched junctions. The shadings are the same in both the tile and the sticky ends of the junction, indicating that the sticky ends on a branched junction can emulate a Wang tile. **(C)** Components of a cumulative XOR calculation. TX tiles are shown as rectangles ending in sticky ends represented geometrically. The input *x* tiles are shown at the upper left, and the value of the tile is shown in the central domain. Initiator tiles C1 and C2 are shown in the upper right and the four possible *y* tiles are shown in the bottom row. The inputs of the *y* tiles is shown on their bottom domains. **(D)** Self-assembled tiles. The strand structure of the TX tiles is illustrated on the upper left, with the reporter strand drawn with a thicker line. The assembly of tiles in a prototype calculation is shown, using the components illustrated in (C). The input 1, 1, 1, 0 produces an output of 1, 0, 1, 1 by successive binding of *y* tiles into the double sites created as the array assembles.

suggested by Winfree ***(4)***, who noticed that the system described above, branched junctions with sticky ends, could be a way to implement computation by "Wang tiles" on the molecular scale. This is a system of tiles whose edges may contain one or more different markings; the tiles self-assemble into a mosaic according to the local rule that all edges in the mosaic are flanked by the same marking. Such a form of assembly can be shown to emulate the operation of a Turing machine, a general-purpose computer ***(46)***. A group of Wang tiles is shown on the left of **Fig. 12A**, and an assembly of Wang tiles is shown on the right. The relationship between the sticky ends of a branched junction and the markings on a Wang tile is shown in **Fig. 12B**.

This form of DNA-based computation has been prototyped successfully in a 4-bit cumulative exclusive OR (XOR) calculation ***(47)***. The XOR calculation yields a 1 if the two inputs are different, and a 0 if they are the same. **Figure 12C** shows the components of this calculation. Each component is a TX molecule, schematized as three rectangles with geometrical shapes on their ends to represent complementarity. The input bits are "*x*" tiles (upper left), and the output bits are "*y*" tiles (bottom), and there are two initiator tiles, C1 and C2, as well (upper right). The upper left corner of **Fig. 12D** shows the strand structure of the TX tiles; each strand contains a "reporter strand" (drawn with a thicker line); the value of *x* and *y* tiles is set to 0 or 1, depending on whether the tile contains a *Pvu*II or *Eco*RV restriction site, respectively. The y_i tiles perform the gating function; there are four of them, corresponding to the four possible combinations of 0 and 1 inputs. The input involves the bottom domain (**Fig. 12C**). The assembly of periodic arrays discussed in **Subheading 3.** entails competition between correct and incorrect tiles for particular positions; by contrast, the competition here is between correct and partially correct tiles. For example, the $y_{i-1} = 0$ sticky end on the leftmost tile is the same as the y_{i-1} sticky end on the rightmost tile. In the cumulative XOR calculation, $y_i = \text{XOR}\ (x_i, y_{i-1})$. The implementation of this formula is shown in **Fig. 12D**. The x_i tiles and the initiators are given longer sticky ends than the y_i tiles, so they assemble a template first when the tiles are cooled. This creates a double site where the υ_1 tile can bind. This binding creates the double site where the y_2 tile can bind, and so on. When the assembly is complete, the reporter strands are ligated together, creating a long strand that connects the input to the output through the initiator tiles. Partial restriction analysis of the resulting strand reveals that the correct answer is obtained almost exclusively.

6. Conclusion

This chapter discussed the current state of structural DNA nanotechnology, emphasizing the individual components, their assembly into objects and

topological targets as well as into periodic and algorithmic arrays, and their manipulation as nanomechanical devices. Where is the field going? The achievement of several key near-term goals will move structural DNA nanotechnology from an elegant structural curiosity to a system with practical consequences. First among these goals is the extension of array-making capabilities from 2D to 3D, particularly with high order. Likewise, heterologous molecules must be incorporated into DNA arrays, so that the goals both of orienting biological macromolecules for diffraction purposes and of organizing nanoelectronic circuits may be met. DNA nanorobotics awaits the incorporation of the PX-JX_2 device into arrays. Algorithmic 3D assembly will lead ultimately to very smart materials, particularly if combined with nanodevices. Hierarchical systems must ultimately be developed, as well as the combination of arrays with aptamers for sensor applications. The development of self-replicating systems using branched DNA appears today to be somewhat oblique ***(48,49)***, but it nevertheless represents an exciting challenge that will significantly economize on the preparation of these systems and increase their development by in vitro evolution. Currently, structural DNA nanotechnology is a biokleptic pursuit, stealing genetic molecules from biological systems; ultimately, it must advance from biokleptic to biomimetic, not just using the central molecules of life, but improving on them, without losing their inherent power as central elements of self-assembled systems.

Acknowledgments

I am grateful to all of my students, postdocs, and collaborators for their contributions to the founding of structural DNA nanotechnology. This research was supported by grants GM-29554 from the National Institute of General Medical Sciences, N00014-98-1-0093 from the Office of Naval Research; DMI-0210844, EIA-0086015, DMR-01138790, and CTS-0103002 from the National Science Foundation, and F30602-01-2-0561 from DARPA/AFSOR.

References

1. Watson, J. D. and Crick, F. H. C. (1953) A structure for deoxyribose nucleic acid. *Nature* **171,** 737–738.
2. Seeman, N. C. (1982) Nucleic acid junctions and lattices. *J. Theor. Biol.* **99,** 237–247.
3. Robinson, B. H. and Seeman, N. C. (1987) The design of a biochip. *Protein Eng.* **1,** 295–300.
4. Winfree, E. (1996) On the computational power of DNA annealing and ligation, in *DNA Based Computing* (Lipton, E. J. and Baum, E. B., eds.), American Mathematical Society, Providence, RI, pp. 199–219.
5. Seeman, N. C. (2000) In the nick of space: generalized nucleic acid complementarity and the development of DNA nanotechnology. *Synlett* **2000,** 1536–1548.

6. Cohen, S. N., Chang, A. C. Y., Boyer, H. W., and Helling, R. B. (1973) Construction of biologically functional bacterial plasmids *in vitro*. *Proc. Nat. Acad. Sci. USA* **70,** 3240–3244.
7. Qiu, H., Dewan, J. C., and Seeman, N. C. (1997) A DNA decamer with a sticky end: the crystal structure of d-CGACGATCGT. *J. Mol. Biol.* **267,** 881–898.
8. Zhang, X., Yan, H., Shen, Z., and Seeman, N. C. (2002) Paranemic cohesion of topologically-closed DNA molecules. *J. Am. Chem. Soc.* **124,** 12,940–12,941.
9. Yan, H. and Seeman, N. C. (2003) Edge-sharing motifs in DNA nanotechnology. *J. Supramol. Chem.* **1,** 229–237.
10. Seeman, N. C. (2001) DNA nicks and nodes and nanotechnology. *Nano Lett.* **1,** 22–26.
11. Holliday, R. (1964) A mechanism for gene conversion in fungi. *Genet. Res.* **5,** 282–304.
12. Fu, T.-J. and Seeman, N. C. (1993) DNA double crossover structures. *Biochem.* **32,** 3211–3220.
13. Schwacha, A. and Kleckner, N. (1995) Identification of double Holliday junctions as intermediates in meiotic recombination. *Cell* **83,** 783–791.
14. LaBean, T., Yan, H., Kopatsch, J., Liu, F., Winfree, E., Reif, J. H., and Seeman, N. C. (2000) The construction, analysis, ligation and self-assembly of DNA triple crossover complexes. *J. Am. Chem. Soc.* **122,** 1848–1860.
15. Yan, H., Zhang, X., Shen, Z., and Seeman, N. C. (2002) A robust DNA mechanical device controlled by hybridization topology. *Nature* **415,** 62–65.
16. Zhang, Y. and Seeman, N. C. (1992) A solid-support methodology for the construction of geometrical objects from DNA. *J. Am. Chem. Soc.* **114,** 2656–2663.
17. Chen, J. and Seeman, N. C. (1991) The synthesis from DNA of a molecule with the connectivity of a cube. *Nature* **350,** 631–633.
18. Zhang, Y. and Seeman, N. C. (1994) The construction of a DNA truncated octahedron. *J. Am. Chem. Soc.* **116,** 1661–1669.
19. Qi, J., Li, X., Yang, X., and Seeman, N. C. (1996) The ligation of triangles built from bulged three-arm DNA branched junctions. *J. Am. Chem. Soc.* **118,** 6121–6130.
20. Hagerman, P. J. (1988) Flexibility of DNA. *Ann. Rev. Biophys. Chem.* **17,** 265–286.
21. Seeman, N. C., Rosenberg, J. M., and Rich, A. (1976) Sequence specific recognition of double helical nucleic acids by proteins. *Proc. Nat. Acad. Sci. USA* **73,** 804–808.
22. Freier, S. M. and Altmann, K.-H. (1997) The ups and down of nucleic acid duplex stability. *Nucleic Acids Res.* **25,** 4229–4243.
23. Nielsen, P. E., Egholm, M., Berg, R. H., and Buchardt, O. (1991) Sequence selective recognition of DNA by strand displacement with a thymine-substituted polyamide. *Science* **254,** 1497–1500.
24. Kallenbach, N. R., Ma, R.-I., and Seeman, N. C. (1983) An immobile nucleic acid junction constructed from oligonucleotides. *Nature* **305,** 829–831.
25. Seeman, N. C. (1990) *De novo* design of sequences for nucleic acid structure engineering. *J. Biomol. Struct. Dynanics* **8,** 573–581.

26. Ma, R. I., Kallenbach, N. R., Sheardy, R. D., Petrillo, M. L., and Seeman, N. C. (1986) Three arm nucleic acid junctions are flexible. *Nucleic Acids Res.* **14,** 9745–9753.
27. Wang, Y., Mueller, J. E., Kemper, B., and Seeman, N. C. (1991) The assembly and characterization of 5-arm and 6-arm DNA junctions. *Biochemistry* **30,** 5667–5674.
28. Petrillo, M. L., Newton, C. J., Cunningham, R. P., Ma, R.-I., Kallenbach, N. R., and Seeman, N. C. (1988) Ligation and flexibility of four-arm DNA junctions. *Biopolymers* **27,** 1337–1352.
29. Eis, P. S. and Millar, D. P. (1993) Conformational distributions of a four-way DNA junction revealed by time-resolved fluorescence resonance energy transfer. *Biochemistry* **32,** 13,852–13,860.
30. Chen, J. and Seeman, N. C. (1991) The electrophoretic properties of a DNA cube and its sub-structure catenanes. *Electrophoresis* **12,** 607–611.
31. Seeman, N. C. (1992) The design of single-stranded nucleic acid knots. *Mol. Eng.* **2,** 297–307.
32. Du, S. M., Stollar, B. D., and Seeman, N. C. (1995) A synthetic DNA molecule in three knotted topologies. *J. Am. Chem. Soc.* **117,** 1194–1200.
33. Mao, C., Sun, W., and Seeman, N. C. (1997) Assembly of Borromean rings from DNA. *Nature* **386,** 137–138.
34. Li, X., Yang, X., Qi, J., and Seeman, N. C. (1996) Antiparallel DNA double crossover molecules as components for nanoconstruction. *J. Am. Chem. Soc.* **118,** 6131–6140.
35. Sa-Ardyen, P., Vologodskii, A. V., and Seeman, N. C. (2003) The flexibility of DNA double crossover molecules. *Biophys. J.* **84,** 3829–3837.
36. Winfree, E., Liu, F., Wenzler, L. A., and Seeman, N. C. (1998) Design and self-assembly of two-dimensional DNA crystals. *Nature* **394,** 539–544.
37. Liu, F., Sha, R., and Seeman, N. C. (1999) Modifying the surface features of two-dimensional DNA crystals. *J. Am. Chem. Soc.* **121,** 917–922.
38. Mao, C., Sun, W., and Seeman, N. C. (1999) Designed two-dimensional DNA Holliday junction arrays visualized by atomic force microscopy. *J. Am. Chem. Soc.* **121,** 5437–5443.
39. Sha, R., Liu, F., Millar, D. P., and Seeman, N. C. (2000) Atomic force microscopy of parallel DNA branched junction arrays. *Chem. Biol.* **7,** 743–751.
40. Sha, R., Liu, F., and Seeman, N. C. (2002) Atomic force measurement of the inter-domain angle in symmetric Holliday junctions. *Biochemistry* **41,** 5950–5955.
41. Yang, X., Vologodskii, A. V., Liu, B., Kemper, B., and Seeman, N. C. (1998) Torsional control of double stranded DNA branch migration. *Biopolymers* **45,** 69–83.
42. Rich, A., Nordheim, A., and Wang, A. H.-J. (1984) The chemistry and biology of left-handed Z-DNA. *Ann. Rev. Biochem.* **53,** 791–846.
43. Mao, C., Sun, W., Shen, Z., and Seeman, N. C. (1999) A DNA nanomechanical device based on the B-Z transition. *Nature* **397,** 144–146.
44. Yurke, B., Turberfield, A. J., Mills, A. P. Jr., Simmel, F. C., and Neumann, J. L. (2000) A DNA-fuelled molecular machine made of DNA. *Nature* **406,** 605–608.

45. Adleman, L. (1994) Molecular computation of solutions to combinatorial problems. *Science* **266,** 1021–1024.
46. Grünbaum, B. and Shephard, G. C. (1986) *Tilings & Patterns*, Freeman, New York.
47. Mao, C., LaBean, T., Reif, J. H., and Seeman, N. C. (2000) Logical computation using algorithmic self-assembly of DNA triple crossover molecules. *Nature* **407,** 493–496.
48. Seeman, N. C. (1991) The construction of 3-D stick figures from branched DNA. *DNA Cell Biol.* **10,** 475–486.
49. Eckardt, H. E., Naumann, K., Pankau, W. M., Rein, M., Schweitzer, M., Windhab, N., and von Kiedrowski, G. (2002) Chemical copying of connectivity. *Nature* **420,** 286.